A belief function model for pixel data

John Klein and Olivier Colot

Abstract Image data *i.e.* pixel values are notably corrupted with uncertainty. A pixel value can be seen as uncertain because of additional noise due to acquisition conditions or compression. It is possible to represent a pixel value in a more imprecise but less uncertain way by considering it as interval-valued instead of a single-valued. The Belief Function Theory (BFT) allows to handle such interval-based pixel representations. We provide in this paper a model describing how to define belief functions from image data. The consistency of this model is demonstrated on edge detection experiments as conflictual pixel-based belief functions lead to image transitions detection.

1 Introduction

The Belief Function Theory (BFT) [3, 8], also known as evidence theory or Dempster-Shafer theory, provides a framework for processing uncertain and imprecise data. As image data can be considered as such, an evidential model leading to a new representation of pixel values can be introduced. Existing evidential image processing approaches are mainly dedicated to information fusion on multiple image components or neighbor pixels as part of pixel classification algorithms [1, 10]. In this article, we intend to process images using the BFT under a new perspective by introducing a model that translates directly each raw pixel value into a belief function. Indeed, a pixel value equals x with probability p. It is also possible to consider that the pixel value belongs to the interval $[x-q,x+q]$ with a probability $p' > p$ and $q > 0$. This piece of information can be easily encoded using a belief function.

John Klein
Lille1 University, LAGIS FRE CNRS 3303, e-mail: john.klein@univ-lille1.fr

Olivier Colot
Lille1 University, LAGIS FRE CNRS 3303, e-mail: olivier.colot@univ-lille1.fr

In section 2, BFT fundamental concepts necessary for our approach are recalled. Section 3 presents a methodology to represent pixel values as belief functions. Section 4 introduces results for pixel conflict computation. Finally, in section 5, the consistency of the model is demonstrated through edge detection experiments on synthetic gray-scale images.

2 Belief functions fundamentals

In this section, BFT fundamentals are briefly recalled. The BFT provides a formal framework for dealing with both imprecise and uncertain data. The finite set of mutually exclusive solutions is denoted by $\Omega = \{\omega_1, ..., \omega_K\}$ and is called the **frame of discernment**. The set of all subsets of Ω is denoted by 2^Ω. A source S_i collects pieces of evidence leading to the assignment of belief masses to some elements of 2^Ω. The mass of belief assigned to A by S_i is denoted $m_i(A)$. The function $m_i : 2^\Omega \rightarrow [0,1]$ is called **basic belief assignment** (**bba**) and is such that: $\sum_{A \subseteq \Omega} m_i(A) = 1$.
A set A such that $m_i(A) > 0$ is called a **focal element** of m_i. A bba is denoted by ${}^A m^x$ if it has two focal elements: Ω and $A \subsetneq \Omega$, and if:

$$ {}^A m^x(A) = 1 - x \text{ and } {}^A m^x(\Omega) = x. \tag{1}$$

with $x \in [0,1]$. Such bbas are called **simple bbas** (sbbas). The bba denoted by ${}^A m^0$, or simply ${}^A m$, stands for the certainty that the truth belongs to A. Thus, ${}^\Omega m$ stands for total ignorance (${}^\Omega m(\Omega) = 1$); it is called the **vacuous bba**. To combine bbas issued by reliable sources, the conjunctive rule $\textcircled{\cap}$ can be used:

$$ \forall X \in 2^\Omega, m_{1\textcircled{\cap}2}(X) = \sum_{B,C|B\cap C=X} m_1(B) m_2(C). \tag{2}$$

The mass $m(\emptyset)$ is denoted by κ and called the **degree of conflict**. This mass is given support when S_1 and S_2 advocate respectively for non-intersecting solutions. It is thus an indication on how much the two sources disagree.

Furthermore, it is possible to reduce the impact of a source of information and its corresponding bba using an operation called discounting [8]. This can be required for several reasons notably if the source of information is known to be unreliable or to enclose perishable information. Discounting m_i with discount rate $\alpha \in [0,1]$ is defined as:

$$ m_i^\alpha(X) = (1-\alpha) m_i(X) + \alpha \mathbf{1}_{X=\Omega} \tag{3}$$

with $\mathbf{1}$ the indicator function. The higher α is, the stronger the discounting. Thanks to discounting, a source's bba is transformed into a function closer to the vacuous bba and $m_i^1 = {}^\Omega m$. One may remark that a sbba ${}^A m^x$ is ${}^A m$ discounted with rate x.

3 A model for pixel representation using belief functions

In this section, our evidential pixel representation (EPR) model is introduced. Let us denote a pixel $\mathbf{p} = (p_x, p_y)$ with p_x and p_y its coordinates along the two image axes. An 8-bit gray-scale image can be represented by a function $I(\mathbf{p})$ such that $0 \leq I(\mathbf{p}) \leq 255$.
The measured image $\tilde{I}$ can be viewed as the sum of the true image and a random noise B: $\tilde{I} = I + B$, and $B(\mathbf{p}) \sim f_b$ the noise density function. Suppose one is able to find a cumulative distribution function F such that $\forall q, F(q) \geq F_b(q) = \int_{-\infty}^{q} f_b(v)\,dv$, then the following assertion holds:

$$1 - 2F(-q) \leq \mathbb{P}\left(\text{true pixel value } I(\mathbf{p}) \in \left[\tilde{I}(\mathbf{p}) - q, \tilde{I}(\mathbf{p}) + q\right]\right) \leq 1 \tag{4}$$

For example, in case of a Gaussian centered noise, F is simply the cumulated density of a centered Gaussian function with a greater standard deviation than that of f_b. Now, by choosing $\Omega = \{0, ..., 255\}$, the set of integers between 0 and 255, this information on a pixel value is represented by the following parametrized bba $m_{\mathbf{p},q}$:

$$m_{\mathbf{p},q} = {}^{\left[\tilde{I}(\mathbf{p})-q, \tilde{I}(\mathbf{p})+q\right]}m^{2F(-q)} \tag{5}$$

Multiple bbas may be defined by this mean, as it is difficult to determine what value for q to choose. Because the image is quantized, the set of possible values for q is $Q = \{0.5, 1.5, ..., 255.5\}$. These values yield intervals of width 1, 3 and so long up to 511. The focal sets drawn from these intervals are their intersections with Ω. Building a bba with $q = 255.5$ is only interesting when the pixel value is 0 or 255. For other pixel values, we have $m_{\mathbf{p},255.5} = {}^{\Omega}m$ (vacuous bba). To cumulate all pieces of evidence, we propose to define the bba representing pixel $\mathbf{p}$ as the conjunctive combination of parametrized bbas for all possible values of q:

$$m_{\mathbf{p}} = \bigcirc\!\!\!\!\!\!\bigcap_{q \in Q} m_{\mathbf{p},q}. \tag{6}$$

A frequent criticism addressed to the BFT is the computational load induced by large frames of discernment. In this paper, the cardinal of 2^{Ω} is 2^{255}, thus computing the above bba using equation (2) is infeasible. Yet, since the set of bbas to combine has some particular properties, this computation can be easily done using the following proposition:

Theorem 1. *Let $\left\{m_i = {}^{A_i}m^{\alpha_i}\right\}_{i=1}^{N}$ be a set of sbbas with focal elements such that $A_1 \subsetneq A_2 \subsetneq ... \subsetneq A_N \subsetneq \Omega$. Let us denote $m_{\bigcirc\!\!\!\!\!\!\bigcap}$ the conjunctive combination of these sbbas. We have:*

$$m_{\bigcirc\!\!\!\!\!\!\bigcap}(X) = (1 - \alpha_i) \prod_{j=1}^{i-1} \alpha_j \mathbf{1}_{X=A_i} + \prod_{j=1}^{N} \alpha_j \mathbf{1}_{X=\Omega} \tag{7}$$

Proof. The focal elements of $m_{\bigcirc\!\!\!\!\!\!\bigcap}$ are the sets $\{A_i\}_{i=1}^{N}$ and Ω. For $\{A_i\}_{i=1}^{N}$, we have:

$$m_{\textcircled{\cap}}(A_i) = \sum_{\cap_{j=1}^{N} B_j = A_i, B_j \subset \Omega} {}^{A_1}m^{\alpha_1}(B_1) \ldots {}^{A_N}m^{\alpha_N}(B_N)$$

The condition under the sum can only be verified if $\forall j < i, B_j = \Omega$ and $B_i = A_i$. Since ${}^{A_i}m^{\alpha_i}(A_i) = (1-\alpha_i)$ and $\forall j < i$, ${}^{A_j}m^{\alpha_j}(\Omega) = \alpha_j$, we have:

$$m_{\textcircled{\cap}}(A_i) = (1-\alpha_i)\prod_{j=1}^{i-1}\alpha_j \sum_{\cap_{j=i+1}^{N} B_j \cap A_i = A_i, B_j \subset \Omega} {}^{A_{i+1}}m^{\alpha_{i+1}}(B_{i+1}) \ldots {}^{A_N}m^{\alpha_N}(B_N)$$

The condition remaining under the sum is always verified because $\forall j > i, A_i \cap A_j = A_i$. Therefore, we have: $m_{\textcircled{\cap}}(A_i) = (1-\alpha_i)\prod_{j=1}^{i-1}\alpha_j$.
Finally, the mass allocated to Ω is easily obtained from more general results about the conjunctive rule: $\forall m_i, m_j$, $m_i \textcircled{\cap} m_j(\Omega) = m_i(\Omega)\, m_j(\Omega)$. □

Note that, if one draws this way two bbas $m_{\mathbf{p}}$ and $m_{\mathbf{p}'}$ for two different pixels with identical intervals width q, then we have $\forall i$, $m_{\mathbf{p}}(A_i) = m_{\mathbf{p}'}(A'_i) = \beta_i$. The masses of these bbas are always the same, only the focal sets differ.

4 Pixel conflict computation

In the previous section, we have obtained bbas $m_{\mathbf{p}}$ representing uncertain and imprecise values of each pixel. We present now a simple way to compute pixel-based degree of conflict.
As mentioned before, the cardinality of Ω makes it hard to compute the degree of conflict using equation (2). To overcome this difficulty, we propose to use a result from [4]. It is shown in that article that if there is at least one pairwise positive degree of conflict among a set of bbas $\{m_i\}_{i=1}^{M}$, then the global conflict of a set of identically discounted bbas can be approximated by the sum of pairwise degrees of conflict. Consequently, it is semantically equivalent to compute the global degree of conflict or the sum of pairwise degrees of conflict, as identically discounting bbas preserves their relative prevalences. The pairwise conflict of two bbas $m_{\mathbf{p}}$ and $m_{\mathbf{p}'}$ can be easily computed using the following result:

Theorem 2. *Let $m_{\mathbf{p}}$ and $m_{\mathbf{p}'}$ be two bbas obtained from the process described in section 3. Then their pairwise conflict $\kappa_{\{\mathbf{p},\mathbf{p}'\}}$ is a function of $\Delta = \left|\tilde{I}(\mathbf{p}) - \tilde{I}(\mathbf{p}')\right|$ and*

$$\kappa_{\{\mathbf{p},\mathbf{p}'\}}(\Delta) = \begin{cases} \kappa_{\{\mathbf{p},\mathbf{p}'\}}(\Delta-1) + 2\sum_{k=1}^{\Delta/2}\beta_k\beta_{\Delta-k} \text{ if } \Delta \text{is even}, \\ \kappa_{\{\mathbf{p},\mathbf{p}'\}}(\Delta-1) + 2\sum_{k=1}^{(\Delta-1)/2}\beta_k\beta_{\Delta-k} + \beta^2_{(\Delta+1)/2} \text{ if } \Delta \text{is odd}, \end{cases} \tag{8}$$

Proof. If one denotes by k the index of a focal element of $m_{\mathbf{p}}$ and by l the index of a focal element of $m_{\mathbf{p}'}$, those with empty intersections are such that $k+l \leq \Delta$. Conse-

quently, we obtain $\kappa_{\{\mathbf{p},\mathbf{p}'\}} = \sum_{k+l\leq\Delta} \beta_k\beta_l$. It can be seen that $\kappa_{\{\mathbf{p},\mathbf{p}'\}}$ is a function of Δ which can be recursively computed. Indeed, we have $\kappa_{\{\mathbf{p},\mathbf{p}'\}}(\Delta) - \kappa_{\{\mathbf{p},\mathbf{p}'\}}(\Delta-1) = \sum_{k+l=\Delta} \beta_k\beta_l$. In the end, some elements of $\sum_{k+l=\Delta} \beta_k\beta_l$ are counted twice that is why two cases are distinguished corresponding odd and even values of Δ. □

The values of β_i for all i and of $\kappa_{\{\mathbf{p},\mathbf{p}'\}}(\Delta)$ for all Δ can be stored in a lookup table, making it easy and fast to compute pixel pairwise degrees of conflict. The method appears to be based only on pixel value differences. The function applied to these differences is entirely justified using the BFT and is based on conflict.

5 Experiments on edge detection

The degree of conflict of bbas belonging to the neighborhood $\mathcal{V}_\mathbf{p}$ of pixel $\mathbf{p}$ is obtained as follows: $\kappa(\mathbf{p}) = \sum_{\mathbf{p}'\in\mathcal{V}_\mathbf{p}} \kappa_{\{\mathbf{p},\mathbf{p}'\}}$. It is likely to be a relevant feature for assessing the presence of an edge at pixel $\mathbf{p}$. Consequently, edge detection was chosen to demonstrate the consistency of EPR. For using the EPR, one must first define function F. The unkown noise f_b is supposed to be centered and Gaussian. The function F is thus defined likewise with a greater standard deviation σ_{EPR} than that of the noise. A pixel neighborhood $\mathcal{V}_\mathbf{p}$ is defined as follows: $\mathcal{V}_\mathbf{p} = \left\{\mathbf{p}' | \sqrt{(p_x - p'_x)^2 + (p_y - p'_y)^2} \leq h_{EPR}\right\}$. An edge dectector yields a binary edge image whereas $\kappa(\mathbf{p})$ corresponds to an image containing edge probabilities (if normalized). If $\kappa(\mathbf{p})$ appraises correctly image edges, then it should be compliant with output edge probability distributions drawn from classical edge detection algorithms. The algorithms retained for the experiments are : Roberts [7], Prewitt [6], Sobel [9], Canny [2] and LoG [5] edge detectors. Roberts, Prewitt and Sobel detectors are based on image first derivatives whereas LoG is based on second order derivatives. Canny [2] introduced a filter as an optimal solution in terms of detection of step edges, edge localization and uniqueness. In addition to filtering, his approach also comprises two other steps helping to obtain thin edges and to remove false edges. To allow a fair comparison of the methods, we only use in the experiments the filtering part of Canny's approach.
Roberts, Sobel and Prewitt are parameter-free, but LoG, Canny and $\kappa(\mathbf{p})$ are depending on two parameters each: a filter spread h_{LoG}, h_{Canny}, h_{EPR} respectively and a standard deviation σ_{LoG}, σ_{Canny}, σ_{EPR} respectively. For Canny and LoG, the filter spread is usually greater than at least three times the standard deviation. Concerning h_{EPR}, its value was set to 2 for all experiments. σ_{LoG}, σ_{Canny}, σ_{EPR} are hand-tuned in each experiment. The value yielding the lowest Kullback-Leibler D_{KL} divergence is retained. This criterion is defined as:

$$D_{KL}(I_e||GT) = \sum_\mathbf{p} I_e(\mathbf{p}) \log\left(\frac{I_e(\mathbf{p})}{GT(\mathbf{p})}\right) \tag{9}$$

where I_e is an edge probability image and GT the ground truth. When these distributions are identical $D_{KL}(I_e||GT) = 1$. Higher values are obtained when the distributions are different. This criterion is adapted to our purpose as it penalizes wrongly located edges, thick edges and partially detected edges. Note that a contrast enhancement is used on some of the images displayed in this section in order to help the reader to percieve some image details.

5.1 Omni-directional edges

In this experiment, the dependence on edge direction is examined. A synthetic image I_1 containing a ramp-edge in shape of a circle is used. The edge is made of two transitions: from 0 to gray level 125 and from 125 to 255. When using a step-edge with a single transition from 0 to 255, the edge is located at a subpixel precision which makes it harder to define a ground thruth.
I_1, its corresponding ground truth GT as well as the output edge probability distributions produced by several approaches are presented in Figure 1. The D_{KL} obtained in this experiment are gathered in Table 1. $\kappa(\mathbf{p})$ produces the smallest divergence because the edge distribution is thinner.

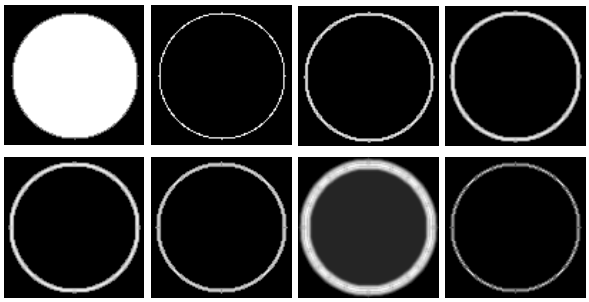

Fig. 1 From top-left to down-right: input image I_1, ground truth GT, output edge distribution using Roberts, Sobel, Prewitt, Canny, LoG and $\kappa(\mathbf{p})$. $\sigma_{Canny} = 0.3$, $\sigma_{LoG} = 0.9$ and $\sigma_{EPR} = 1e5$

Table 1 Performances of several edge detection methods on synthetical image I_1.

Method	Roberts	Sobel	Prewitt	Canny $\sigma_{Canny} = 0.3$	LoG $\sigma_{LoG} = 0.9$	$\kappa(\mathbf{p})$ $\sigma_{EPR} = 1e5$
D_{KL}	8.61	8.32	8.52	7.88	11.56	3.81

5.2 Edges with varying contrast

In this experiment, the dependence on edge contrast is examined. The input image I_2 is obtained by shading I_1. I_2, GT and the edge probability distributions are

presented in Figure 2. The corresponding D_{KL} are gathered in Table 2. $\kappa(\mathbf{p})$ produces the smallest divergence because the transitions inside the circle are filtered out. The divergence is more stringent on this aspect than on detecting the whole circle. Smaller values of σ_{EPR} leads to performances close to Canny's ones.

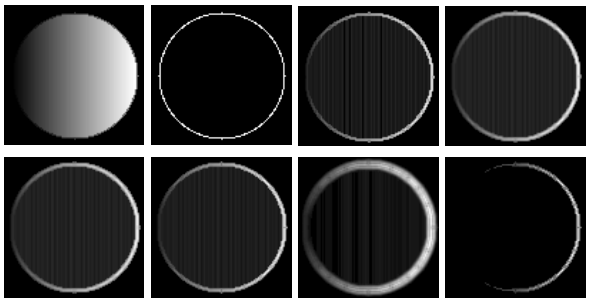

Fig. 2 From top-left to down-right: input image I_2, ground truth GT, output edge distribution using Roberts, Sobel, Prewitt, Canny, LoG and $\kappa(\mathbf{p})$. $\sigma_{Canny} = 0.4$, $\sigma_{LoG} = 0.9$ and $\sigma_{EPR} = 1e5$

Table 2 Performances of several edge detection methods on synthetical image I_2.

Method	Roberts	Sobel	Prewitt	Canny $\sigma_{Canny} = 0.4$	LoG $\sigma_{LoG} = 0.9$	$\kappa(\mathbf{p})$ $\sigma_{EPR} = 1e5$
D_{KL}	9.98	9.70	9.84	9.40	11.82	4.53

5.3 Robustness to Gaussian noise

In this experiment, the robustness to additive Gaussian noise is examined. The input image I_3 is obtained by adding to I_2 such a noise with standard deviation $\sigma_b = 50$. I_3, GT and the edge probability distributions are presented in Figure 3. The corresponding D_{KL} are gathered in Table 3. Again, $\kappa(\mathbf{p})$ produces the smallest divergence because non-relevant transitions are filtered out. Obviously, if the edge distributions were thresholded, Canny's approach would detect a larger part of the circle than $\kappa(\mathbf{p})$. Smaller values of σ_{EPR} lead to output images close to Canny's. It is important to remind that **it is only intended to validate EPR and not to introduce an edge detector**. For such a purpose, additonal experiments involving image thresholding and natural images are needed.

Table 3 Performances of several edge detection methods on synthetical image I_3.

Method	Roberts	Sobel	Prewitt	Canny $\sigma_{Canny} = 1.5$	LoG $\sigma_{LoG} = 1.2$	$\kappa(\mathbf{p})$ $\sigma_{EPR} = 1e5$
D_{KL}	13.31	12.85	12.83	12.28	13.13	12.02

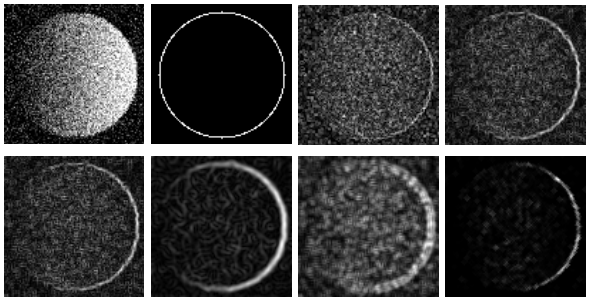

Fig. 3 From top-left to down-right: input image I_3, ground truth GT, output edge distribution using Roberts, Sobel, Prewitt, Canny, LoG and $\kappa(\mathbf{p})$. $\sigma_{Canny} = 1.5$, $\sigma_{LoG} = 1.2$ and $\sigma_{EPR} = 1e5$

6 Conclusion

In this paper, a model for pixel representation (EPR) is proposed. This model is based on the belief function theory. The consistency of this model was proved through preliminary edge detection experiments. Indeed, the degree of conflict of neighbor pixels appears to be a relevant feature to assess the presence of an edge. The approach is easy to implement and and does not require a heavy computation load. The goal behind this paper is to pave the way for future evidential image processing developments. Some additional processes and experiments will be investigated to introduce potentially a full edge detector. Furthermore, the EPR should also be extended to multi-component images and other belief masses than the degree of conflict may be exploited.

References

1. Bloch, I.: Some aspects of dempster-shafer evidence theory for classification of multi-modality medical images taking partial volume effect into account. Pattern Recognition Letters **17**(8), 905 – 919 (1996)
2. Canny, J.: Finding edges and lines in images. Tech. rep., Cambridge, MA, USA (1983)
3. Dempster, A.: A generalization of bayesian inference. Journal of Royal Statistical Society **B 30**, 205–247 (1968)
4. Klein, J., Colot, O.: Singular sources mining using evidential conflict analysis. International Journal of Approximate Reasoning **52**(0), 1433–1451 (2011)
5. Marr, D., Hildreth, E.: Theory of edge detection. Proceedings of the Royal Society of London, Series B, Biological Science **207**(1167), 187–217 (1980)
6. Prewitt, J.: Object enhancement and extraction. Picture Processing and Psychopictorics pp. 75–149 (1970). Academic Press, New York
7. Roberts, L.: Machine perception of 3-D solids. Optical and Electro-optical Information Processing (1965). MIT press
8. Shafer, G.: A Mathematical Theory of Evidence. Princeton University press, Princeton (NJ), USA (1976)
9. Sobel, I.: Camera model and machine perception. Ph.D. thesis, Stanford University (1970)
10. Vannoorenberghe, P., Macaire, L., Colot, O.: Computer Vision Research Progress, chap. 11, Evidence-based pixel labeling for color image segmentation, pp. 279–296. Nova Science (2008)